Polymer 51 (2010) 6346–6354

Contents lists available at ScienceDirect

Polymer

journal homepage: www.elsevier.com/locate/polymer

Reaction-induced microphase separation in polybenzoxazine thermosets containing poly(N-vinyl pyrrolidone)-*block*-polystyrene diblock copolymer

Di Hu, Sixun Zheng*

Department of Polymer Science and Engineering and State Key Laboratory of Metal Matrix Composites, Shanghai Jiao Tong University, Shanghai 200240, PR China

ARTICLE INFO

Article history:
Received 23 July 2010
Received in revised form
11 October 2010
Accepted 23 October 2010
Available online 30 October 2010

Keywords:
Polybenzoxazine
Poly(N-vinyl pyrrolidone)-*block*-polystyrene diblock copolymer
Reaction-induced microphase separation

ABSTRACT

Poly(N-vinyl pyrrolidone)-*block*-polystyrene diblock copolymer (PVPy-*b*-PS) was synthesized *via* sequential reversible radical-fragmentation transfer polymerization with *S*-1-phenylethyl *O*-ethyl-xanthate as a chain transfer agent. The block copolymer was incorporated into polybenzoxazine to access the nanostructures in the thermosets. The nanostructures in the thermosets were investigated by means of transmission electron microscopy (TEM) and small-angle X-ray scattering (SAXS). It was found that disordered and/or ordered PS nanophases were formed in the PBa thermosets. It is judged that the formation of nanophases followed the mechanism of reaction-induced microphase separation in terms of the miscibility of the subchains of the diblock copolymer (*viz.* PVPy and PS) with polybenzoxazine after and before curing reaction.

1. Introduction

During the past decades considerable attention has been paid to the investigations on reaction-induced phase separation (RIPS) in multi-component thermosets [1,2]. The goal of these studies is to establish the correlation of morphology with the properties of materials. The modified thermosets are prepared starting from a homogenous solution of modifier (*e.g.*, thermoplastics or elastomers) with precursors of thermosets and then the fine morphologies are formed by modulating the competitive kinetics between phase separation and polymerization. The driving force of RIPS is ascribed to the decreased entropic contribution to the mixing free energy owing to the occurrence of polymerization (*viz.* cross-linking). Nonetheless, the miscible thermosetting blends can be obtained while there were the favorable intermolecular specific interactions (*e.g.*, hydrogen bonding) between these polymers and thermosets [3–6].

Generally, RIPS takes place on the macroscopic scale since these modifiers are some homopolymers or random copolymers. While the polymeric modifiers are some amphiphilic block copolymers, which contain both thermoset-philic and thermoset-phobic subchains, the RIPS could be confined to the micrometer scale *i.e.*, so-called reaction-induced microphase separation (RIMPS) occurs and thus the nanostructures in thermosets would be obtained [1,2]. Recently, RIMPS has been proved to an efficient alternative to the nanostructures in thermosets [7–15]. In a previous work, Zheng et al. [7] demonstrated that the formation of nanostructures in epoxy thermosets containing poly(ε-caprolactone)-*block*-polybutadiene-*block*- poly(ε-caprolactone) triblock copolymer followed the RIMPS mechanism and RIMPS has been found in a variety of thermosetting blends containing amphiphilic block copolymers [7–16]. It should be pointed out that Bates et al. [17,18] have ever proposed the strategy of self-assembly to access the nanostructures of thermosets. In this protocol, the precursors of thermosets act as the selective solvents of block copolymers and some self-organized nanostructures are formed in the mixtures before curing reaction. These preformed nanostructures are fixed through the subsequent curing reaction. The self-assembly behavior has been extensively investigated during the past decade vis-à-vis RIMPS of block copolymers in thermosetting polymers [9,19–32]. Mechanistically, there is a significant difference between self-assembly and RIMPS approaches. In self-assembly approach, the formation of nanophases is governed by the equilibrium thermodynamics of the multi-component system comprised of precursors of thermosets and amphiphilic block copolymer. Nonetheless, the formation of nanostructures *via* RIMPS could be greatly influenced by the competitive kinetics between polymerization and phase separation. With the reaction proceeding, a series of structural changes involving chain extension, branching and crosslinking occurred in succession, *i.e.*, the system undergoes the sol–gel transition within a short time.

* Corresponding author. Tel.: +86 21 54743278; fax: +86 21 54741297.
E-mail address: szheng@sjtu.edu.cn (S. Zheng).

0032-3861/$ – see front matter © 2010 Elsevier Ltd. All rights reserved.
doi:10.1016/j.polymer.2010.10.047

Benzoxazines (Ba) are a class of bicyclic heterocycle consisting of a benzene ring fused to that of oxazine, which can be prepared *via* Mannich condensation among phenol, formaldehyde and amine [33–48]. Polybenzoxazines (PBa) thermosets can be obtained *via* thermally activated ring-opening polymerization of benzoxazine monomers and no hardeners are required involving the curing process [34–36] (See Scheme 1). PBa thermosetting polymers are a class of novel thermosets and are becoming the promising alternatives to some traditional thermosets such as epoxies, phenolic resins and bismaleimides owing to their excellent thermal, mechanical and electrical properties [33–48]. The potential applications of PBa motivate to prepare their thermosetting blends with improved properties [36–38,49–51]. Chang et al. [49] reported that PBa thermoset was miscible with poly(N-vinyl pyrrolidone) and the miscibility was ascribed to the formation of inter-component hydrogen-bonding interactions. This could be the first report on the fully miscible blends of PBa. The most of PBa thermosetting blends found hereto are phase-separated. Ishida et al. [36] investigated that the synergism in PBa blends containing 0–15 wt% of poly(ε-caprolactone) by means of dynamic mechanical analysis. Fourier transform infrared spectroscopy showed that within the compositions investigated there were the intermolecular hydrogen-bonding interactions between PBa and poly(ε-caprolactone). Zheng et al. have found the occurrence of macroscopic phase separation-induced by reaction in the thermosetting blends of PBa with poly(ε-caprolactone) [50] and the similar results were also reported that in the thermosetting blends of PBa with poly (ethylene oxide) [51]. The reaction-induced phase separation occurred at the micrometer scale since the polymeric modifiers used to prepare the blends were some homopolymers. Recently, it has been recognized that the formation of the nanostructures in the multi-component thermosets can further optimize the interactions between thermosetting matrix and modifiers and thus the mechanical properties of materials were significantly improved, which has been called “toughening by nanostructures” [52]. To the best of our knowledge, however, no precedent works were reported on the formation of nanostructures in PBa thermosets by the use of an amphiphilic diblock copolymer.

The purpose of this work is to demonstrate that disorder and/or ordered nanostructures could be accessed *via* RIMPS approach in the thermosetting blends of PBa by the use of amphiphilic block copolymer. Toward this end, a diblock copolymer, poly(N-vinyl pyrrolidone)-*block*-polystyrene (PVPy-*b*-PS) was used by knowing that PVPy is miscible with PBa thermosets [49] whereas PS will undergo reaction-induced phase separation in PBa thermosets. It is expected that the nanostructured epoxy thermosets can be prepared *via* RIMPS approach. In this work, the PVPy-*b*-PS diblock copolymer was firstly synthesized *via* sequential reversible radical-fragmentation transfer (RAFT) polymerization approach and then transmission electron microscopy (TEM) and small-angle X-ray scattering (SAXS) are used to examine the nanostructures in the thermosets. The formation mechanism of nanostructures is judged on the basis of the miscibility of subchain with the thermoset after and before curing reaction.

2. Experimental

2.1. Materials

4,4′-Dihydroxyldiphenylisopropane, aniline, 1-bromoethylbenzene and carbon disulfide were of analytical pure grade, purchased from Shanghai Reagent Co., China. Paraformaldehyde was obtained from Aldrich Co., USA. Styrene was purchased from Shanghai Reagent Co., Shanghai, China and the inhibitor was eliminated by washing thrice using aqueous solution of sodium hydroxide (5%) and the monomer was dried with anhydrous magnesium sulfate before it was distilled under decreased pressure. N-vinyl-2-pyrrolidone was obtained from Acros Co., Shanghai, China. and used as received. The solvents such as chloroform and toluene were obtained from commercial source and they were purified with standard procedures prior to use. Benzoxazine was synthesized by following the approach of literature on the basis of Mannich condensation among 4,4′-dihydroxyldiphenylisopropane, aniline and paraformaldehyde with toluene as the solvent [33].

2.2. Synthesis of S-1-phenylethyl O-ethylxanthate

To a 150 ml flask anhydrous ethanol (20 ml) and potassium hydroxide (2.8 g, 0.05 mol) were charged with vigorous stirring until a transparent solution was obtained. The flask was immersed into ice-water bath and carbon disulfide (10 ml) was slowly dropped and the reaction was allowed to carry out at room temperature for 10 h. The excess carbon disulfide was distilled out at 70 °C and then 1-bromoethylbenzene (5.66 ml, 0.0413 mol) dissolved in 10 ml ethanol was added into the mixture and the reaction was performed at 60 °C for 5 h. The solids (*viz*. inorganic salts) in the system were removed *via* filtration and then ethyl ether (20 ml) and deionized water (20 ml) were added. The solution was washed with deionized water thrice and the organic layer was collected and dried with anhydrous magnesium sulfate. After filtration the

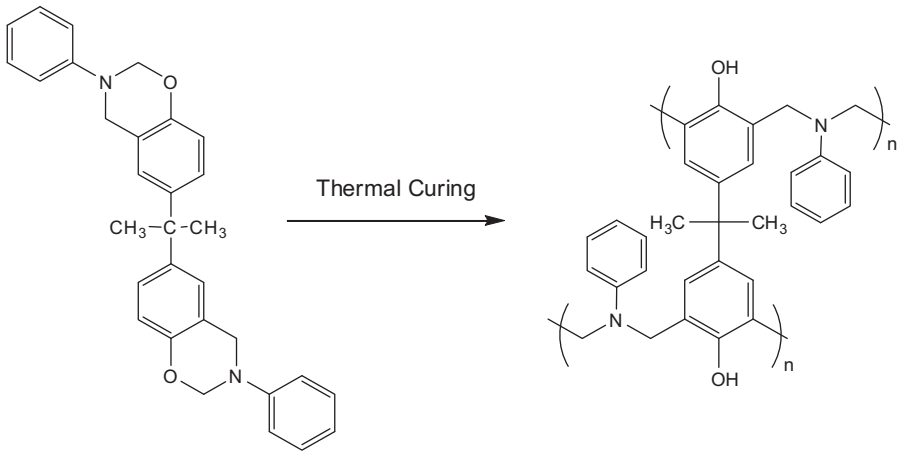

Scheme 1. Thermal curing of Ba monomer.

solvents were eliminated *via* rotary evaporation and yellow oil liquid (8.61 g) was obtained with the yield of 76.2% after drying *in vacuo* at 30 °C for 30 h. ^{1}H NMR ($CDCl_3$, ppm): 1.39 (3H, $C\boldsymbol{H}_3CH_2$), 1.72(3H, $C\boldsymbol{H}_3CH$), 4.62 (2H, $CH_3C\boldsymbol{H_2}$), 4.91 (1H, $CH_3C\boldsymbol{H}$), 7.27–7.40 (5H, $C_6\boldsymbol{H}_5$).

2.3. Synthesis of polystyrene macromolecular chain transfer agent (PS-CTA)

To a 50 ml flask styrene (15.0 g, 0.14 mol), *S*-1-phenylethyl *O*-ethylxanthate (15.0 g, 0.14 mol), azodiisobutyronitrile (AIBN) (0.0371 g, 0.22 mmol) and anhydrous toluene (2.4 ml) were charged. The system was connected to a Schlenk line and the reactive mixture was degassed *via* three pump freeze–thaw cycles and then immersed in a thermostated oil bath at 80 °C for 26 h. The crude product was dissolved in tetrahydrofuran and the solution was dropped into a great amount of methanol to afford the precipitates and this procedure was repeated three times. The precipitates were dried *in vacuo* at 30 °C for 24 h. By controlling the conversion of monomer the product (10.18 g) was obtained with the yield of *c.a.* 66.2%. The molecular weight of the macromolecular chain transfer agent (PS-CTA) was estimated to be M_n = 8900 in term of the molar ratio of monomer (at the conversion of 66.2%) to the RAFT agent (*i.e.*, *S*-1-phenylethyl *O*-ethylxanthate). ^{1}H NMR ($CDCl_3$, ppm): 6.19–7.23 (5H, $C_6\boldsymbol{H}_5$ of polystyrene), 1.44 (1H, $C\boldsymbol{H}_2CHC_6H_5$), 1.85 (2H, $CH_2C\boldsymbol{H}C_6H_5$). GPC: M_n = 9100, M_w/M_n = 1.51.

2.4. Synthesis of poly(N-vinyl pyrrolidone)-block-polystyrene diblock copolymer

N-vinyl pyrrolidone (3.4600 g, 30 mmol), PS-CTA (2.0005 g, 0.22 mmol), 1,4-dioxane (4 ml) and AIBN (0.0092 g, 0.05 mmol) were charged to a 50 ml flask. The flask was connected to a Schlenk line and the reactive mixture was degassed *via* three pump freeze–thaw cycles and then immersed in a thermostated oil bath at 70 °C for 26 h. The crude product was dissolved in tetrahydrofuran and the solution was dropped into a great amount of petroleum to afford the precipitates. This procedure was repeated three times and the precipitates were dried *in vacuo* at 30 °C for 24 h. By controlling the conversion of monomer the product (3.2 g) was obtained with the yield of *c.a.* 36.7%. The length of the PVPy block was estimated to be M_n = 5500 in term of the molar ratio of monomer (at the conversion of 46.7%) to the PS-CTA. ^{1}H NMR ($CDCl_3$, ppm): 6.19–7.23 (8.3H, C_6H_5 of polystyrene), 2.15–2.55 [2H, $NCH_2CH_2C\boldsymbol{H}_2CO$], 3.75 [1H,$C\boldsymbol{H}N(CH_2)_3CO$], 3.24 [2H, $NC\boldsymbol{H}_2CH_2CH_2CO$], 1.2–2.13 (methylene protons as indicated by the peaks *a, b, h* and *e* in Fig. 1). Gel permeation chromatography (GPC): M_n = 15,200 with M_w/M_n = 1.57.

2.5. Preparation of Ba and PS blends

The blends of Ba with the model PS were prepared by solution casting from tetrahydrofuran at room temperature. The concentration was controlled within 5% (w/v). To remove the residual solvent, all the blend films were further desiccated *in vacuum* at 50 °C for 48 h.

2.6. Preparation of PBa thermosets containing PVPy-b-PS

The desired amount of diblock copolymer PVPy-*b*-PS was dissolved in the smallest amount of tetrahydrofuran and the solution was added to Ba with continuous stirring until the homogenous solution was obtained. Before curing reaction, the majority of solvent was evaporated at 60 °C for 2 h and the residual solvent was eliminated *in vacuo* at 30 °C for 2 h. The mixtures were poured into Teflon molds and cured at 180 °C for 4 h. The contents of the diblock copolymer in the PBa thermosets were controlled to be 10, 20, 30 and 40 wt%, respectively.

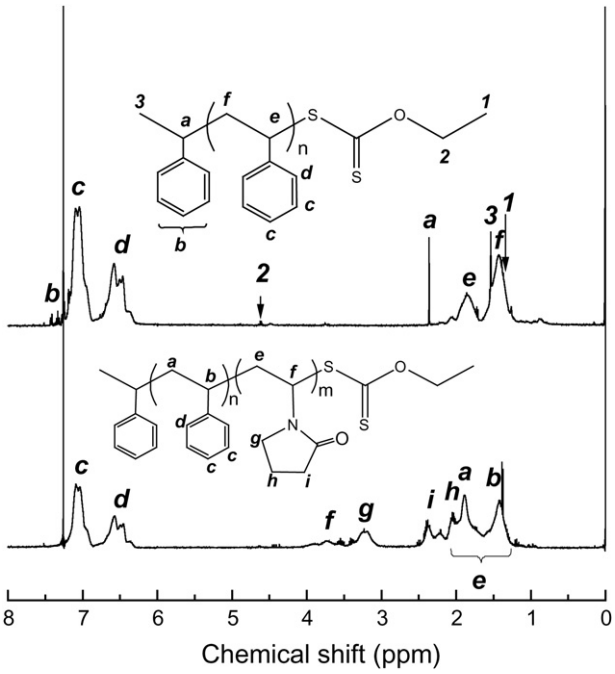

Fig. 1. ^{1}H NMR spectrum of PS-CTA and PVPy-*b*-PS diblock copolymer.

2.7. Measurement and characterization

2.7.1. Fourier transform infrared spectroscopy (FTIR)

FTIR measurement was carried out on a Perkin–Elmer Paragon 1000 Fourier transform spectrometer. For the measurement of the PVPy-*b*-PS diblock copolymer, the trace of water in the polymer was eliminated *via* azeotropic distillation technique. The block copolymer (0.1 g) was dissolved in 20 ml anhydrous toluene and 10 ml solvent was distilled out and then the solution of the diblock copolymer was cast onto KBr windows at 60 °C and the residual solvent was removed *in vacuo* at 60 °C for 1 h. For the samples of thermosets, the powder was mixed with KBr pellets to press into small flakes. All the specimens were sufficiently thin to be within a range where the Beer–Lambert law is obeyed. In all cases 64 scans at a resolution of 2 cm^{-1} were used to record the spectra.

2.7.2. Nuclear magnetic resonance spectroscopy (NMR)

The samples were dissolved in deuteronated chloroform and the NMR spectra were measured on a Varian Mercury Plus 400 MHz NMR spectrometer with tetramethylsilane (TMS) as the internal reference.

2.7.3. Gel permeation chromatography (GPC)

The molecular weights and molecular weight distribution of polymers were determined on Waters 717 Plus autosampler gel permeation chromatography apparatus equipped with Waters RH columns and a Dawn Eos (Wyatt Technology) multi-angle laser light scattering detector and the measurements were carried out at 25 °C with tetrahydrofuran (THF) as an eluent at the rate of 1.0 ml/min.

2.7.4. Atomic force microscopy (AFM)

The specimens of thermosets for AFM observation were trimmed using a microtome machine and the thickness of the

specimens is about 70 nm. The morphological observation of the samples was conducted on a Nanoscope IIIa scanning probe microscope (Digital Instruments, Santa Barbara, CA) in tapping mode. A tip fabricated from silicon (125 μm in length with *ca.* 500 KHz resonant frequency) was used for scan, and the scan rate was 2.0 Hz.

2.7.5. Transmission electron microscopy (TEM)

Transmission electron microscopy (TEM) was performed on a JEOL JEM-2010 transmission electron microscope at an acceleration voltage of 200 kV. The samples were trimmed on a microtome machine with a diamond knife and the sections of the samples were stained with 5% RuO_4 aqueous solution for 20 min to increase the contrast. The stained specimen sections with the thickness of 70–100 nm in thickness were placed in 200 mesh copper grids for observations.

2.7.6. Small-angle X-ray scattering (SAXS)

The SAXS measurements were taken on a small-angle X-ray scattering station (BL16B1) with a long-slit collimation system in the Shanghai Synchrotron Radiation Facility (SSRF), Shanghai, China, in which the third generation of synchrotron radiation light sources was employed. Two dimensional diffraction patterns were recorded using an image intensified CCD detector. The experiments were carried out with the radiation of X-ray with the wavelength of $\lambda = 1.24$ Å at room temperature (25 °C). The intensity profiles were output as the plot of scattering intensity (I) versus scattering vector, $q = (4/\lambda) \sin(\theta/2)$ (θ = scattering angle).

2.7.7. Differential scanning calorimetry (DSC)

The calorimetric measurements were performed on a Perkin–Elmer Pyris 1 differential scanning calorimeter in a dry nitrogen atmosphere. An indium standard was used for temperature and enthalpy calibrations, respectively. The samples (about 10.0 mg in weight) were first heated to 140 °C and held at this temperature for 3 min to remove the thermal history, followed by quenching to −40 °C. A heating rate of 20 °C/min was used in all cases. Glass transition temperature (T_g) was taken as the midpoint of the heat capacity change.

2.7.8. Scanning electron microscope (SEM)

In order to observe the phase structure of PBa blends, the samples were fractured under cryogenic condition using liquid nitrogen. The fractured surfaces so obtained were immersed in tetrahydrofuran at room temperature for 30 min. The PS phases could be preferentially etched by the solvent while epoxy matrix phase remains unaffected. The etched specimens were dried to remove the solvents. The fracture surfaces were coated with thin layers of gold of *c.a.* 100 Å. All specimens were examined with a Hitachi S210 scanning electron microscope (SEM) at an activation voltage of 20 kV.

3. Results and discussion

3.1. Synthesis of PVPy-b-PS diblock copolymer

It has ever been a challenge to synthesize well-defined PVPy block copolymer *via* living radical polymerization techniques owing to the high reactivity of N-vinyl pyrrolidone [53]. Under the normal conditions of living radical polymerization, the polymerization of such an unconjugated monomer can give rise to the loss of controllability in living radical polymerization and the occurrence of several side reactions such as disproportionation and chain transfer to form dead polymers. Therefore, some measures of deactivation must be taken to perform the living radical polymerizations of N-vinyl pyrrolidone [54]. By organostilbine-mediated living radical polymerization [55], Yamago et al. have reported the synthesis of poly(N-vinyl pyrrolidone)-*block*-polystyrene (PVPy-*b*-PS). Arsalani et al. [56] synthesized PVPy-*b*-PS diblock copolymer by nitroxide-mediated living free radical polymerization. More recently, Hussain et al. [57] reported the synthesis of diblock copolymers of polystyrene (PS) and poly(N-vinyl pyrrolidone) (PVPy) by a combination of the atom transfer radical polymerization and macromolecular design *via* interchange of xanthates (*i.e.,* ATRP/MADIX). In this work, the RAFT/MADIX process [57] was used to obtain the PVPy-*b*-PS diblock copolymer. The route of synthesis is shown in Scheme 2 and a two-step sequential reversible radical-fragmentation transfer (RAFT) polymerization approach was employed. *S*-1-Phenylethyl-*O*-ethylxanthate was used as the chain transfer agent [58,59]. In the first step, the polystyrene macromolecular chain transfer agent (PS-CTA) was prepared *via* the RAFT polymerization with the desired conversion of styrene. In this work, the conversion of styrene was controlled to be 66.2% to obtain the molecular weight of PS-CTA to be $M_n = 8900$, which is quite close to the value measured by means of GPC (*i.e.*, $M_n = 9100$ with $M_w/M_n = 1.51$).

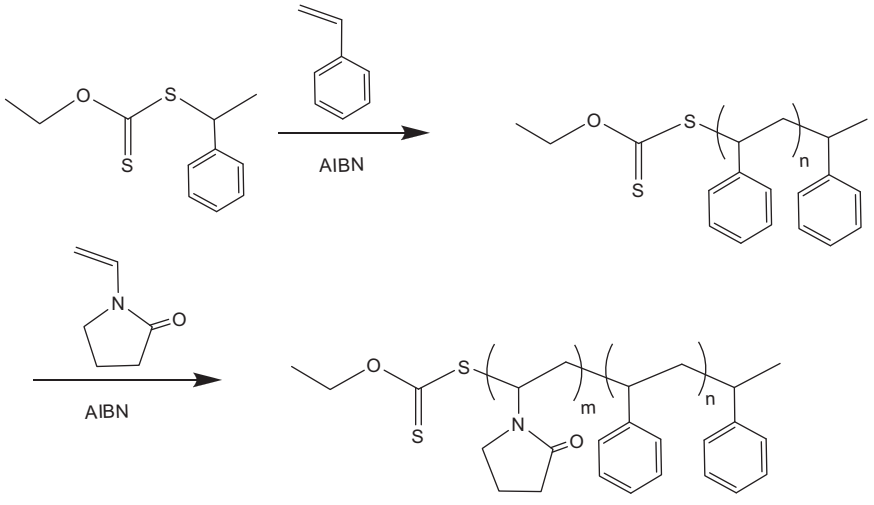

Scheme 2. Synthesis of poly(*N*-vinyl pyrrolidone)-*block*-polystyrene (PVPy-*b*-PS) diblock copolymer.

The PS-CTA was used to polymerize N-vinyl pyrrolidone with AIBN as the initiator. By controlling the conversion of N-vinyl pyrrolidone, the PVPy-*b*-PS diblock copolymer was obtained with the length of PVPy subchain to be $M_n = 5500$. Shown in Fig. 1 are the ^{1}H nuclear magnetic resonance spectra of PS-CTA and the PVPy-*b*-PS diblock copolymer. The PS block was the characteristic of the signals at 1.44, 1.85 and 6.0–8.0 ppm, which are assignable to the resonance of protons of methylene, methane and aromatic ring, respectively. It is worth noticing that the signals of CTA are discernible at 1.35, 1.71, 2.36 and 7.30–7.5 ppm, which are attributed to the protons of methyl, methylene and aromatic rings, respectively. In the ^{1}H NMR spectrum of PVPy-*b*-PS diblock copolymer, the signals from methylene groups of pyrrolidone ring were detected at 3.2, 2.4 and 2.1 ppm, which are ascribed to the protons of methylene groups connected to nitrogen atom, carbonyl groups and those between these two methylene groups, respectively. In addition, the resonance of protons for the methane of PVPy main-chain was detected at 3.72 ppm. The ^{1}H NMR spectroscopy indicates that the PS-CTA and PVPy-*b*-PS diblock copolymer with designed structures were successfully obtained. Both PS-CTA and PVPy-*b*-PS diblock copolymer were subjected to gel permeation chromatography (GPC) and the curves of GPC are presented in Fig. 2. It is seen that the GPC curves of PS-CTA and PVPy-*b*-PS diblock copolymer displayed unimodal peaks. The polymerization of N-vinyl pyrrolidone with the PS-CTA as chain transfer agent did not yield detectable unreacted PS-CTA in the resulting diblock copolymer. The molecular weight of the diblock copolymer was determined to be $M_n = 15{,}200$ with the polydispersity of $M_w/M_n = 1.57$, which was slightly higher than that of PS-CTA. The polydispersity of the diblock copolymer is quite close to the results reported by other investigators [57]. The results of ^{1}H NMR and GPC indicate that the PVPy-*b*-PS diblock copolymer was successfully obtained.

3.2. Nanostructures of PBa thermosets containing PVPy-b-PS

The PVPy-*b*-PS diblock copolymer was incorporated into polybenzoxazine to access the nanostructures in the thermosets. Before curing, all the binary mixtures composed of benzoxazine and PVPy-*b*-PS diblock copolymer were homogenous and transparent. After cured at 180 °C for 4 h, the PBa thermosets were obtained with the content of PVPy-b-PS diblock copolymers up to 40 wt%. All the thermosets were homogenous and transparent, implying that macroscopic phase separation did not take place with the curing reaction. Nonetheless, the reaction-induced microphase separation (RIMPS) cannot be excluded only in view of the clarity. The morphology of PBa thermosets containing PVPy-*b*-PS diblock copolymer was examined by means of transmission electron microscopy (TEM) and small-angle X-ray scattering (SAXS).

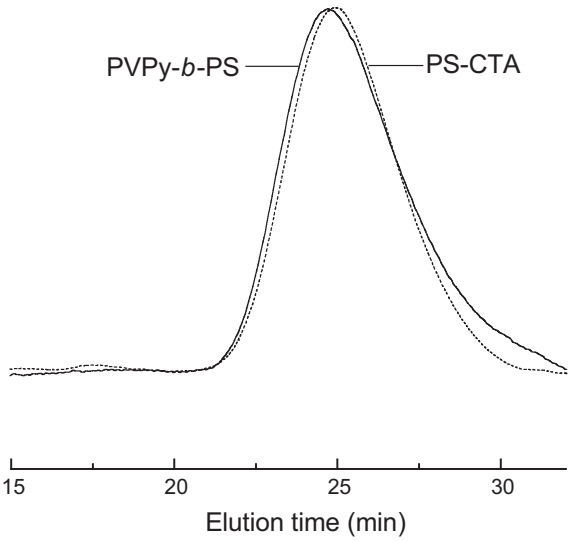

Fig. 2. GPC curves of PS-CTA and PVPy-*b*-PS diblock copolymer.

The PBa thermosets containing PVPy-*b*-PS diblock copolymer were trimmed using an ultra-thin microtome machine and the specimens were subjected to the morphological observations by means of TEM. In order to increase the contrast the sections of the samples were then stained with RuO_4, the PBa matrix containing PVPy can be deeply stained whereas PS microdomains were only lightly stained. Shown in Fig. 3 are the TEM micrographs of the thermosets containing 10, 20, 30 and 40 wt % PVPy-*b*-PS diblock copolymer. It is noted that all the thermosetting blends possess microphase-separated morphologies (*i.e.,* nanostructures). The dark continuous regions are assignable to the PBa matrix, which was miscible with the PVPy subchains of the block copolymer whilst the light regions are attributed to PS domains. While the contents of PVPy-*b*-PS are 10 and 20 wt%, the spherical PS nanophases were imbedded in the continuous PBa matrix at the average size of *c.a.* 20–30 nm in diameter (Fig. 3A and B). With increasing the content of PVPy-*b*-PS diblock copolymer, the number of PS nanodomains increased (Fig. 3B). While the content of PVPy-*b*-PS diblock copolymer is 30 wt% or higher, the PS nanodomains became increasingly interconnected and some cylindered nanophases were exhibited (See Fig. 3C and D). It is of interest to note that the PS nanophases were to some extent arranged into ordered structures. The order of the nanostructures increased with increasing the concentration of PVPy-*b*-PS diblock copolymer. The ordered nanostructures were further investigated by means of SAXS.

The SAXS profiles of the thermosets containing 10, 20, 30, and 40 wt% of PVPy-*b*-PS diblock copolymer are shown in Fig. 4. It is seen that the well-defined scattering peaks were observed in all the cases, indicating that the PBa thermosets containing PVPy-*b*-PS were indeed microphase-separated. According to the position of the primary scattering peaks, the principal domain spacing d_m can be obtained to be 55.6, 51.0, 43.6, and 41.9 nm for the thermosets containing 10, 20, 30 and 40 wt % PVPy-*b*-PS diblock copolymer, respectively. It is noted that except for the thermoset containing 10 and 20 wt% of PVPy-*b*-PS diblock copolymer the thermosetting blends displayed the multiple scattering maxima, indicating that the materials possessed long-range ordered nanostructures. The scattering peaks of the thermosets situated at q values of 1, $4^{0.5}$ and $9^{0.5}$ relative to the first-order scattering peak positions (q_m) are discernable. It is proposed that these are the scattering peaks of cylindrical nanophases arranged in hexagonal lattices. In addition, body-centered (or face-centered) cubic lattice is also possible. It should be pointed out that it is not easy unambiguously to judge the types of packing lattices only in terms of SAXS profiles for the thermosetting blends containing 30, 40 wt% PVPy-*b*-PS since the scattering peaks are quite broad, *i.e.*, the ordering is apparently not good enough. Nonetheless, it is noted that in the thermosetting blends the local rearrangement owing to the increase in the concentration of PVPy-*b*-PS diblock copolymer leads to an enhancement of the long-range order.

3.3. Formation mechanism of nanostructures

It has been recognized that the formation of nanostructures in thermosets by the use of amphiphilic block copolymers could

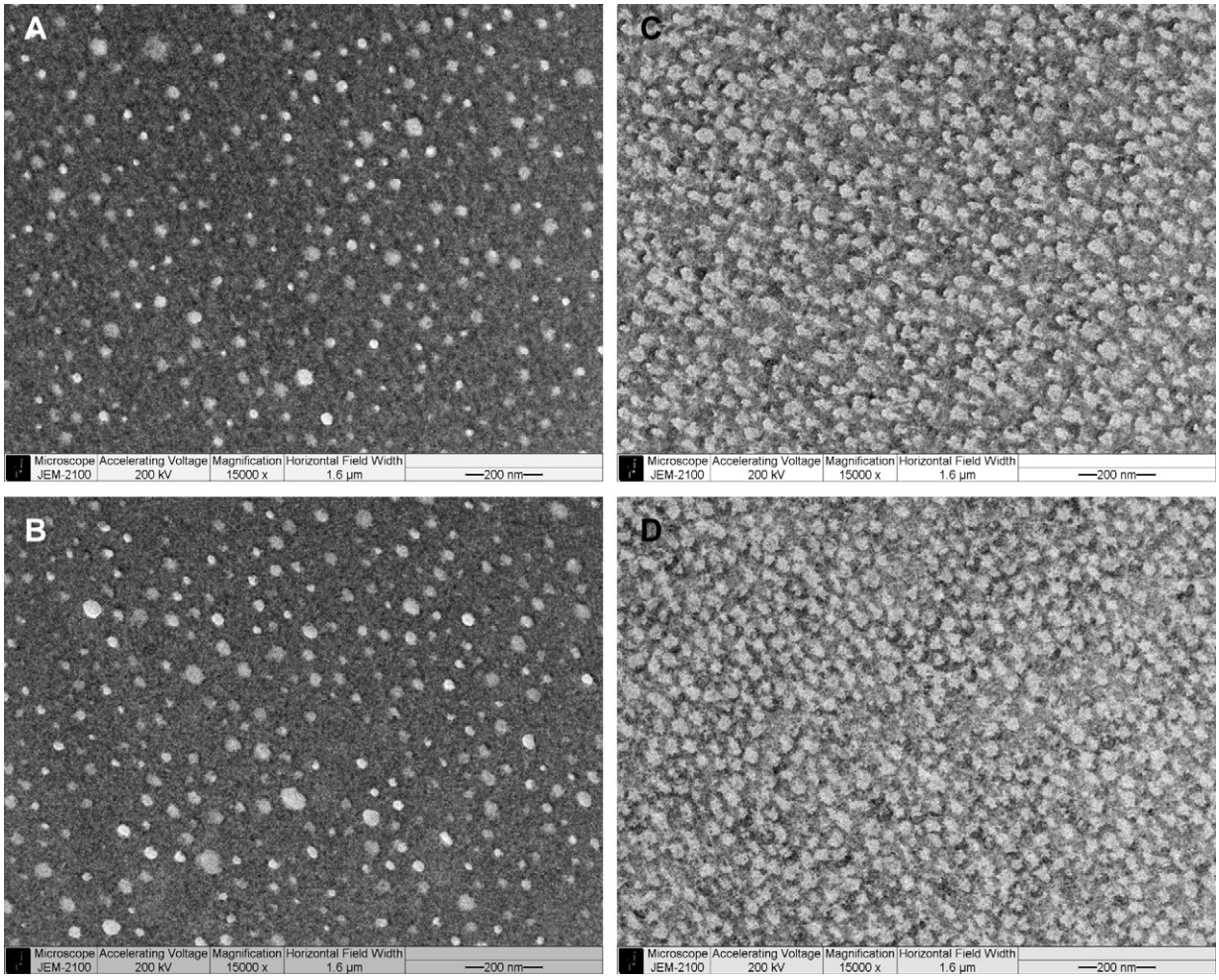

Fig. 3. TEM micrograph of PBa thermoset containing: A) 10, B) 20, C) 30 and D) 40 wt% PVPy-*b*-PS diblock copolymer. The sections of samples were stained with RuO_4.

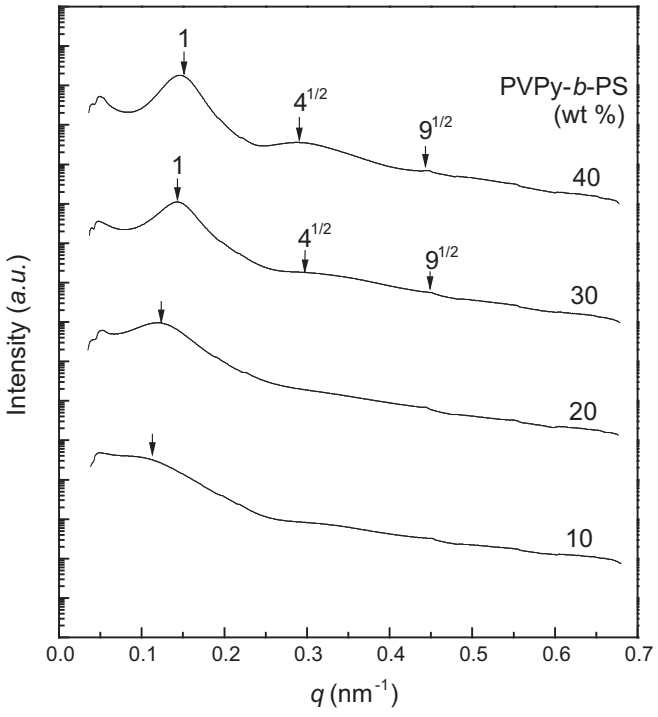

Fig. 4. SAXS curves of the PBa thermosets containing PVPy-*b*-PS diblock copolymer.

follow either self-assembly [17,18] or reaction-induced microphase separation mechanism [7,8]. For the mechanism of self-assembly, the precursors of thermosets act as selective solvents of block copolymers and self-organized nanophases (*i.e.*, micelle) are formed prior to curing and these nanostructures are further locked in with subsequent curing reaction. For reaction-induced microphase separation mechanism, it is not required that the amphiphilic block copolymers are self-organized into the nanophases before curing reaction, *i.e.*, all the subchains of block copolymers may be miscible with precursors of thermosets. Upon curing, a part of subchains of block copolymers are demixed to form the microphases whereas other subchains of the block copolymer remain mixed with the matrix of thermosets. In the present case, it is important to know the miscibility and phase behavior in the blends of the subchains of diblock copolymers with PBa after and before curing reaction for the judgment of the formation mechanism of the nanostructures. The miscibility of Ba and PVPy blends has been previously reported by Chang et al. [49] and it has been demonstrated that the thermosetting blends of PBa and PVPy were miscible after and before curing. Before curing reaction, the miscibility of PVPy with Ba monomer is ascribed to the non-negligible contribution of mixing entropy (ΔS_m) to mixing free energy (ΔS_m) since the molecular weight of Ba monomer is quite low. The miscibility of PBa thermosets with PVPy was attributed to the formation of intermolecular hydrogen-bonding interactions between PVPy and the PBa networks.

Thermally activated ring-opening polymerization of benzoxazine monomers affords the PBa networks which bear a great amount of phenolic hydroxyl groups (See Scheme 1). These phenolic hydroxyl groups are potential to form the intermolecular hydrogen-bonding interactions with the pyrrolidone rings, which are readily investigated by means of Fourier transform infrared spectroscopy (FTIR). Shown in Fig. 5 are the FTIR spectra of control PBa and the nanostructured PBa thermosets in the range of 3000–3800 cm^{-1}. The bands in this region are assignable to the stretching vibration of phenolic hydroxyl groups. For control PBa, a broad band centered at 3437 cm^{-1} is ascribed to the stretching vibration of hydrogen-bonded phenolic hydroxyl groups [60]. Upon adding PVPy-*b*-PS diblock copolymer to the thermoset, a shoulder band at 3373 cm^{-1} appeared. The intensity of the shoulder band increased with increasing the content of PVPy-*b*-PS diblock copolymer. The new band is assignable to the phenolic hydroxyl groups which were associated with pyrrolidone ring of PVPy subchains, *i.e.,* the intermolecular hydrogen-bonding interactions between PBa matrix and PVPy subchains were formed. The observation that the stretching vibration of phenolic hydroxyl groups partially shifted to the lower frequencies indicates that the intermolecular hydrogen-bonding interactions between the phenolic hydroxyl groups and the pyrrolidone rings are much stronger than the self-associations of the phenolic hydroxyl groups [49,61–63]. The intermolecular hydrogen-bonding interactions can be further evidenced by the change of infrared bands for the carbonyl groups of pyrrolidone rings. Shown in Fig. 6 are the FTIR spectra of PVPy-*b*-PS diblock copolymer and the nanostructured PBa thermosets in the range of 1600–1760 cm^{-1}. For PVPy-*b*-PS diblock copolymer, the infrared band in this region of frequency is ascribed to the stretching vibration of amide groups in pyrrolidone ring. The quite broad band reflects the broad distribution of frequencies assignable to free and dipole–dipole interacted pyrrolidone rings, respectively [63,64]. Upon adding PBa to PVPy-*b*-PS diblock copolymer two shoulder bands at 1687 and 1650 cm^{-1} are increasingly discernible. It is plausible to propose that the component at the higher frequency is ascribed to free pyrrolidone rings whereas that at the lower frequency could be attributed to the pyrrolidone rings which are hydrogen-bonded with the phenolic hydroxyl groups of PBa networks. Table 1 summarizes the results of curve-fitting [62,63,66,67] for the PVPy-*b*-PS diblock copolymer and the nanostructured PBa thermosets containing PVPy-*b*-PS diblock copolymer. It is seen that the fractions of the H-bonded and free carbonyl groups increased with increasing the content of PBa in the thermosets, indicating that the pyrrolidone rings were H-bonded with the phenolic hydroxyl groups of PBa networks. The slight increase in the quantity of free pyrrolidone ring could be ascribed to the restriction of crosslinked PBa networks on the conformation of PVPy chains. The FTIR spectroscopy indicates that the PVPy subchains are intimately mixed with the PBa matrix.

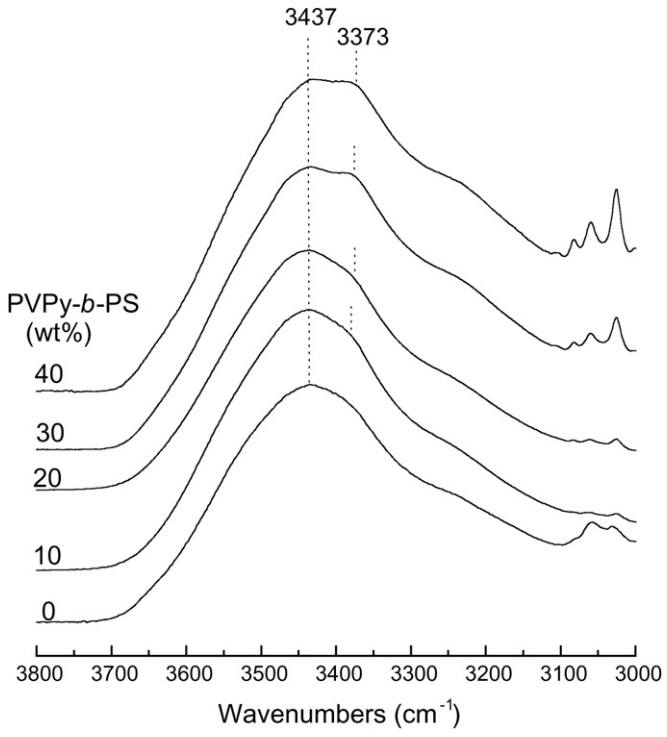

Fig. 5. FTIR spectra of PBa and the PBa thermosets containing PVPy-*b*-PS diblock copolymers.

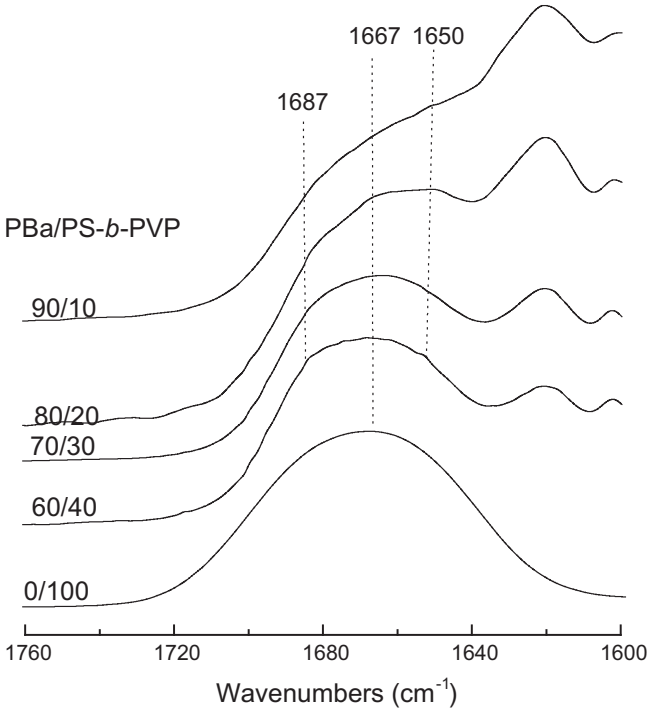

Fig. 6. FTIR spectra of PVPy-*b*-PS and the PBa thermosets containing PVPy-*b*-PS diblock copolymers.

The miscibility and phase behavior of Ba with PS before and after curing reaction were investigated by means of differential scanning calorimetry (DSC) and scanning electron microscopy (SEM), respectively. The model PS having the identical molecular weight with the length of PS in the PVPy-*b*-PS diblock copolymer was used to prepare the PS and Ba blends. The uncured blends were subjected to thermal analysis and the DSC thermograms of the blends were shown in Fig. 7. The Ba monomer displayed the glass transition at 18.3 °C whereas the model PS at 83.8 °C, which is slightly is lower than the value of normal PS (T_g = 100 °C) owing to its lower molecular weight (M_n = 8900). It is seen that each blend exhibited a single T_g and the T_g's of the blends were intermediate between those of plain Ba and PS and decreased with increasing the content of Ba as shown in Fig. 8. The T_g-composition relationship was accounted for by Gordon–Taylor equation [65]:

Table 1
Curve-fitting results of the spectral line in the range of 1638–1760 cm^{-1} for PVPy-b-PS diblock copolymer and the nanostructured PBa thermosets containing PVPy-*b*-PS diblock copolymer.

PVPy-*b*-PS (wt%)	Free carbonyl band			Self-associated carbonyl band			H-bond carbonyl band		
	ν (cm^{-1})	width	area (%)	ν (cm^{-1})	width	area (%)	ν (cm^{-1})	width	area (%)
100	1687	25	8.8	1666	54	91.2	–	–	–
40	1687	25	9.2	1667	54	64.8	1650	54	26.0
30	1687	25	8.9	1666	54	57.2	1650	54	33.9
20	1687	25	11.0	1666	54	29.9	1650	54	59.2
10	1687	25	12.3	1668	54	10.5	1648	54	78.7

$$T_g = T_{g1} + k(W_2/W_1)(T_{g2} - T_g) \quad (1)$$

where T_g is the glass transition temperature of the blends, and the T_{g1} and T_{g2} are those of the blend components. W_i is the weight fraction. The k is an adjusting parameter related to the degree of curvature of the T_g-composition curve. The application of Gordon–Taylor equation to the experimental data yielded a k value of 0.34, fitting the experimental data quite well. The behavior of single and composition-dependent T_g's indicates that the blends of Ba with the model PS are completely miscible. The homogenous mixtures of Ba with the model PS was cured at elevated temperature to obtain the binary blend of PBa with PS. It was observed that with the curing reaction proceeding the transparent and homogenous mixture gradually became cloudy, implying that the reaction-induced phase separation occurred. The cured blends were subjected to the morphological observation by means of scanning electron microscopy (SEM). Before measurement, the fractured end of the sample was etched with tetrahydrofuran to rinse the PS phase whereas the matrix of PBa remained unaffected. Shown in Fig. 9 is the SEM micrograph of the thermosetting blend containing 10 wt% PS. It is seen that some spherical PS particles at the size of 0.2–2.0 μm in diameter were dispersed into the continuous PBa matrix, *i.e.*, a heterogeneous morphology was exhibited. The result of SEM confirmed that the reaction-induced phase separation occurred in the thermosetting blends of PBa with PS.

According to the miscibility of Ba monomer with PVPy and PS blocks, it is proposed that the curing reaction will start from the homogenous solutions composed of Ba and PVPy-*b*-PS diblock copolymer. This speculation has been further confirmed by the fact that no scattering peaks were displayed on the SAXS profiles (not shown) of the mixtures of Ba monomer with PVPy-*b*-PS diblock copolymer. In views of the difference in miscibility and phase behavior in the blends of the subchains (*i.e.*, PS and PVPy) of the diblock copolymer with PBa after and before curing, it is judged that the formation of the nanostructures in PBa thermosets containing PVPy-*b*-PS diblock copolymer followed the mechanism of reaction-induced microphase separation, *i.e.*, at the beginning of the curing reaction, all the subchains (*viz.* PVPy and PS) of the diblock copolymer are miscible with Ba monomer. With the curing reaction proceeding, the PS subchains were separated out at the nanometer scale whereas the PVPy subchains remained mixed with PBa networks *via* the intermolecular hydrogen-bonding interactions.

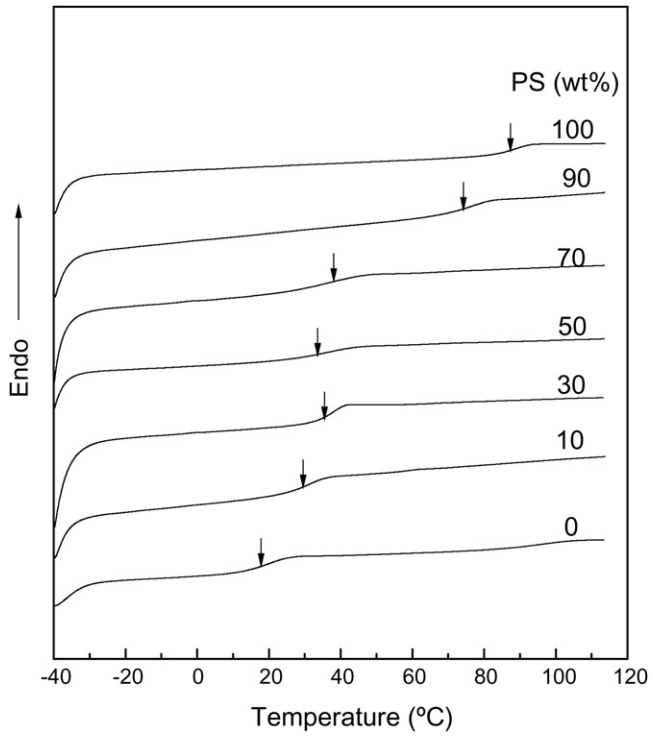

Fig. 7. DSC curves of the blends of Ba monomer with the model PS.

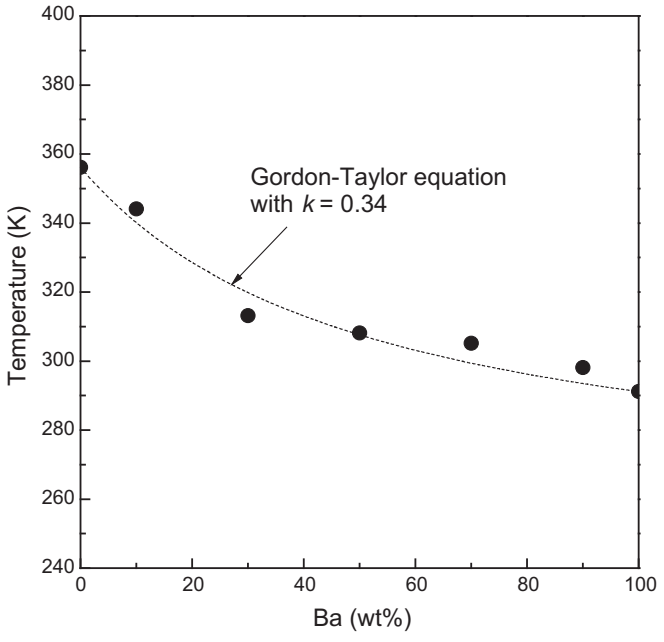

Fig. 8. Plot of glass transition temperatures (T_g's) of the binary mixtures of Ba with the model PS as a function of PS content.

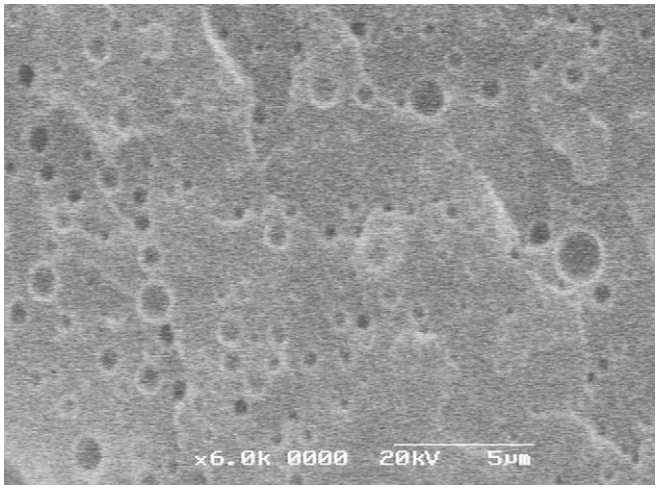

Fig. 9. SEM micrograph of the PBa blend containing 10 wt% of the model PS. The surface was etched with tetrahydrofuran.

4. Conclusions

Poly(N-vinyl pyrrolidone)-*block*-polystyrene (PVPy-*b*-PS) diblock copolymer was synthesized *via* sequential reversible radical-fragmentation transfer polymerization with *S*-1-phenylethyl *O*-ethyl-xanthate as a chain transfer agent. The block copolymer was incorporated into polybenzoxazine to access the nanostructures in the thermosets. It was found that disordered and/or ordered PS nanophases were formed whereas PVPy subchains remained miscible with the PBa thermosets with the occurrence of curing reaction. It is judged that the formation of nanophases followed the mechanism of reaction-induced microphase separation in terms of the miscibility of the subchains of the diblock copolymer (*viz*. PVPy and PS) with polybenzoxazine after and before curing reaction.

Acknowledgment

Financial support from Natural Science Foundation of China (No. 20474038 and 50873059) and National Basic Research Program of China (No. 2009CB930400) is gratefully acknowledged. The authors thank the Shanghai Synchrotron Radiation Facility under the project of 08sr0157 and Shanghai Leading Academic Discipline Project (Project Number: B202) for partial support.

References

[1] Pascault JP, Williams RJJ. In: Paul DR, Bucknall CB, editors. Polymer blends, vol. 1. New York: Wiley; 2000. p. 379–415.
[2] Zheng S. In: Pascault JP, Williams RJJ, editors. Epoxy polymers: new materials and innovations. Weinheim: Wiley-VCH; 2010. p. 79–108.
[3] Noshay A, Robeson LM. J Polym Sci Part A Polym Chem 1974;12:689.
[4] Luo X, Zheng S, Zhang N, Ma D. Polymer 1994;35:2619.
[5] Zheng S, Zhang N, Luo X, Ma D. Polymer 1995;36:3609.
[6] Zheng S, Zheng H, Guo Q. J Polym Sci Part B Polym Phys 2003;41:1085.
[7] Meng F, Zheng S, Zhang W, Li H, Liang Q. Macromolecules 2006;39:711.
[8] Meng F, Zheng S, Li H, Liang Q, Liu T. Macromolecules 2006;39:5072.
[9] Serrano E, Tercjak A, Kortaberria G, Pomposo JA, Mecerreyes D, Zafeiropoulos NE, et al. Macromolecules 2006;39:2254.
[10] Meng F, Zheng S, Liu T. Polymer 2006;47:7590.
[11] Sinturel C, Vayer M, Erre R, Amenitsch H. Macromolecules 2007;40:2532.
[12] Ocando C, Serrano E, Tercjak A, Pena C, Kortaberria G, Calberg C, et al. Macromolecules 2007;40:4068.
[13] Xu Z, Zheng S. Macromolecules 2007;40:2548.
[14] Meng F, Xu Z, Zheng S. Macromolecules 2008;41:1411.
[15] Fan W, Wang L, Zheng S. Macromolecules 2009;42:327.
[16] Ocando C, Tercjak A, Martín MD, Ramos JA, Campo M, Mondragon I. Macromolecules 2009;42:6215.
[17] Hillmyer MA, Lipic PM, Hajduk DA, Almdal K, Bates FS. J Am Chem Soc 1997;119:2749.
[18] Lipic PM, Bates FS, Hillmyer MA. J Am Chem Soc 1998;120:8963.
[19] Mijovic J, Shen M, Sy JW, Mondragon I. Macromolecules 2000;33:5235.
[20] Grubbs RB, Dean JM, Broz ME, Bates FS. Macromolecules 2000;33:9522.
[21] Guo Q, Thomann R, Gronski W. Macromolecules 2002;35:3133.
[22] Ritzenthaler S, Court F, Girard-Reydet E, Leibler L, Pascault JP. Macromolecules 2002;35:6245.
[23] Ritzenthaler S, Court F, Girard-Reydet E, Leibler L, Pascault JP. Macromolecules 2003;36:118.
[24] Rebizant V, Abetz V, Tournihac T, Court F, Leibler L. Macromolecules 2003;36:9889.
[25] Dean JM, Verghese NE, Pham HQ, Bates FS. Macromolecules 2003;36:9267.
[26] Rebizant V, Venet AS, Tournillhac F, Girard-Reydet E, Navarro C, Pascault JP, et al. Macromolecules 2004;37:8017.
[27] Thio YS, Wu J, Bates FS. Macromolecules 2006;39:7187.
[28] Ocando C, Serrano E, Tercjak A, Pena C, Kortaberrića G, Calberg C, et al. Macromolecules 2007;40:4086.
[29] Maiez-Tribut S, Pascault JP, Souleć ER, Borrajo J, Williams RJJ. Macromolecules 2007;40:1268.
[30] Gong W, Zeng K, Wang L, Zheng S. Polymer 2008;49:3318.
[31] Yi F, Zheng S, Liu T. J Phys Chem B 2009;113:11831.
[32] Hu D, Xu Z, Zeng K, Zheng S. Macromolecules 2010;42:2960.
[33] Ning X, Ishida H. J Polym Sci Part A Polym Chem 1994;32:1121.
[34] Kim HJ, Zdenka B, Ishida H. Polymer 1999;40:1815.
[35] Kim HD, Brunovska Z, Ishida H. Polymer 1999;40:6565.
[36] Ishida H, Lee Y-H. Polymer 2001;42:6971.
[37] Ishida H, Lee Y-H. J Polym Sci Part B Polym Phys 2001;39:736.
[38] Takeichi T, Agag T, Zeidam R. J Polym Sci Part A Polym Chem 2001;39:2633.
[39] Agag T, Takeichi T. Macromolecules 2001;34:7257.
[40] Tekeichi T, Zeidam R, Agag T. Polymer 2002;43:45.
[41] Agag T, Tsuchiya H, Takeichi T. Polymer 2004;45:7903.
[42] Ghosh NN, Kiskan B, Yagci Y. Prog Polym Sci 2007;32:1344.
[43] Brunovska Z, Liu J. Macromol Chem Phys 1999;200:1745.
[44] Su Y-C, Chen W-C, Ou K-L, Chang F-C. Polymer 2005;46:3758.
[45] Liu Y, Zheng S. J Polym Sci Part A Polym Chem 2006;44:1168.
[46] Lee Y-J, Kuo S-W, Su Y-C, Chen J-K, Tu C-W, Chang F-C. Polymer 2004;45:6321.
[47] Lee Y-J, Kuo S-W, Huang C-F, Chang F-C. Polymer 2006;47:4378.
[48] Velez-Herrera P, Doyama K, Abe H, Ishida H. Macromolecules 2008;41:9704.
[49] Su Y-C, Kuo S-W, Yei D-R, Xu H, Chang F-C. Polymer 2003;44:2187.
[50] Zheng S, Han L, Guo Q. Macromol Chem Phys 2004;205:1547.
[51] Han L, Zheng S. Polymer 2003;44:4689.
[52] Ruiz-Perez L, Royston GJ, Fairclough JP, Pyan AJ. Polymer 2008;49:4475.
[53] Kirsh YE. Water soluble poly-N-vinylamides, synthesis and physicochemical properties. Chichester: John Wiley & Sons; 1998.
[54] Perrier S, Takolpuckdee P. J Polym Sci Part A Polym Chem 2005;43:5347.
[55] Ray B, Kotani M, Yamago S. Macromolecules 2006;39:5259.
[56] Arsalani N, Fattahi H, Entezami AA. Iran Polym J 2006;15:997.
[57] Hussain H, Tan BH, Gudipati CS, Liu Y, He CB, Davis TP. J Polym Sci Part A Polym Chem 2008;46:5604.
[58] Skey J, O'Reilly RK. Chem Commun; 2008:4183.
[59] Tong Y-Y, Dong Y-Q, Du F-S, Li Z-C. Macromolecules 2008;41:7339.
[60] Kim H-D, Ishida H. Macromolecules 2003;36:8320.
[61] Rothschild WG. J Am Chem Soc 1955;22:3892.
[62] Coleman MM, Graf JF, Painter PC. Specific interactions and the miscibility of polymer blends. Lancaster, PA: Technomic Publishing; 1991.
[63] Coleman MM, Painter PC. Prog Polym Sci 1995;20:1.
[64] Zheng S, Guo Q, Mi Y. J Polym Sci Part B Polym Phys 1999;37:2412.
[65] Gordon M, Taylor JS. J Appl Chem 1952;2:493.
[66] Coleman MM, Lee KH, Shrovanek DJ, Painter PC. Macromolecules 1986;19:2149.
[67] de Ilarduya AM, Iruin JJ, Fernandez-Berridi MJ. Macromolecules 1995;28:3702.